Metal-Assisted Organization of Shortened Carbon Nanotubes in Monolayer and Multilayer Forest Assemblies

Debjit Chattopadhyay, Izabela Galeska, and Fotios Papadimitrakopoulos*

Nanomaterials Optoelectronics Laboratory
Department of Chemistry, Polymer Program
Institute of Materials Science
University of Connecticut, Storrs, Connecticut 06269-3136

Received April 16, 2001

Dense arrays of single-wall carbon nanotubes (SWNTs) aligned normal to substrates has been envisioned to enhance performance of various technologically important devices such as sensors,[1] field emitters,[2] and organic light-emitting diodes.[3] High-temperature catalytic decomposition of hydrocarbon precursors on metal-functionalized substrates have yielded such geometries, however, only multiwall nanotubes (NTs) have been realized thus far.[4,2d] Drawing NT suspensions through a 0.2-μm-pore ceramic filter, while immobilizing the other end on a Teflon substrate, also produced vertically aligned geometries.[5] Shortening SWNTs in an oxidizing environment,[6] followed by chemical modifications of the carboxyl end groups,[6a] presents an alternative method to align the NTs perpendicular to the substrate. Short and long (tens of nm for the shortened SWNTs (s-SWNTs) to a few microns for pristine SWNTs and 1.3−1.4 nm in diameter) SWNTs have exhibited considerable affinity for amine-functionalized substrates, although they tend to orient parallel to the substrate.[6b,c] Thiol functionalization of s-SWNTs resulted in better alignment on gold substrates; nonetheless, this system was plagued by low surface coverage and long adsorption times.[6a] In the present communication we report the formation of dense arrays of s-SWNTs-forest using a metal-assisted self-assembly from nonaqueous media. This approach also permits growth of successive stacks of s-SWNTs, one on top of each other, in a layer-by-layer (LBL) assembly format.

Stable dispersion of largely unbundled s-SWNTs[6b] were obtained by sonicating carboxy-functionalized NTs[7] in DMF using a procedure described elsewhere.[6b] The s-SWNTs assemblies elaborated herein were based on metal-assisted chelation[8] and electrostatic[9] interactions. The self-assembly was performed on substrates such as glass, (100) silicon wafers with native oxide and quartz crystal microbalance (QCM) resonators (9 MHz AT cut; with gold electrodes having a surface area of 0.32 cm^2; USI, Japan). To ensure a smooth and uniformly charged surface, necessary for reproducibility of results, the substrates were modified with polyelectrolyte films via LBL method.[9b,c] s-SWNTs/Fe^{3+} assemblies consisted of sequential dipping in an aqueous solution of $FeCl_3$ (pH 2.2, 15 min) followed by immersion in DMF dispersed s-SWNTs[10] (pH 8.5, typically 30 min) and separated by intermediate washing in DMF (pH 12.7).[11] The elevated pH for both DMF wash and s-SWNTs dispersion causes the surface-immobilized Fe^{3+} layer to transform into its basic hydroxide form,[9a,12] providing the initial driving force (acid−base neutralization) for this assembly to occur (see Scheme 1).

Scheme 1. Schematic Representation of the s-SWNTs Self-Assembly Process

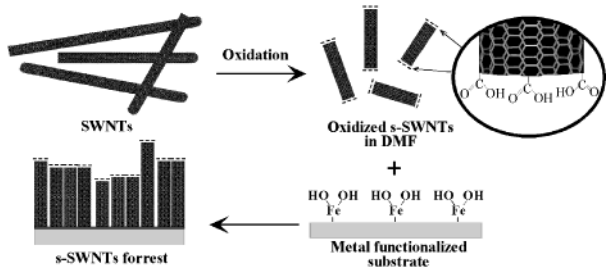

As illustrated in Figure 1, a monolayer of densely packed, needlelike domains is obtained after 30 min immersion in nonaqueous dispersions of s-SWNTs. Although accurate determination of average domain width (93 ± 22 nm) and valley depth might be limited by AFM tip curvature,[13] such morphology is reminiscent of aggregated s-SWNTs, most likely tethered with only one of their ends to the substrate.[6a] This geometry is believed to be the result of (i) high concentration of carboxy groups[14] on the severed edges of s-SWNTs and hydroxy functionalization of Fe^{3+}-decorated surfaces[9a] and (ii) strong hydrophobic interactions between adjacent s-SWNTs.[15] Polarization Raman studies indicate significant orientation normal to the substrate, with a 57-fold intensity enhancement at 1593 cm^{-1}, when polarization of the incident light is parallel to the nanotube axis[21b] (refer to Figure

* To whom correspondence should be addressed: Telephone: (860)-486-3447. Fax: (860)-486-4745. E-mail: papadim@mail.ims.uconn.edu.

(1) (a) Kong, J.; Franklin, N. R.; Zhou, C.; Chapline, G. M.; Peng, S.; Kyeongjae, D.; Hongjie, D. *Science* **2000**, *287*, 622. (b) Collins, P. G.; Bradley, K.; Ishigami, M.; Zettl, A. *Science* **2000**, *287*, 1801.

(2) (a) de Heer, W. A.; Châtelain, A.; Ugarte, D. *Science* **1995**, *270*, 1179. (b) Xu, X.; Brandes, G. R. *Appl. Phys. Lett.* **1999**, *74*, 2549. (c) Rinzler, A. G.; Hafner, J. H.; Nikolaev, P.; Lou, L.; Kim, S. G.; Tománek, D.; Nordlander, P.; Colbert, D. T.; Smalley, R. E. *Science* **1995**, *269*, 1550. (d) Fan, S.; Chapline, M. G.; Franklin, N. R.; Tombler, T. W.; Cassell, A. M.; Dai, H. *Science* **1999**, *283*, 512.

(3) (a) Riggs, J. E.; Guo, Z.; Carroll, D. L.; Sun, Y.-P. *J. Am. Chem. Soc.* **2000**, *122*, 5879. (b) Woo, H. S.; Czerw, R.; Webster, S.; Caroll, D. L.; Ballato, J.; Stevens, A. E.; O'Brien, D.; Blau, W. J. *Appl. Phys. Lett.* **2000**, *77*, 1393.

(4) Ren, Z. F.; Huang, Z. P.; Xu, J. W.; Wang, J. H.; Bush, P.; Siegal, M. P.; Provencio, P. N. *Science* **1998**, *282*, 1105.

(5) de Heer, W. A.; Basca, W. S.; Châtelain, A.; Gerfin, T.; Humpherey-Baker, R.; Forro, L.; Ugarte, D. *Science* **1995**, *270*, 1179.

(6) (a) Liu, Z.; Shen, Z.; Zhu, T.; Hou, S.; Ying, L.; Shi, Z.; Gu, Z. *Langmuir* **2000**, *16*, 3569. (b) Liu, J.; Casavant, M. J.; Cox, M.; Walters, D. A.; Boul, P.; Lu, W.; Rimberg, A. J.; Smith, K. A.; Colbert, D. T.; Smalley, R. E. *Chem. Phys. Lett.* **1999**, *303*, 125. (c) Burghard, M.; Duesberg, G.; Philipp, G.; Muster, J.; Roth, S. *Adv. Mater.* **1998**, *10*, 584.

(7) Liu, J.; Rinzler, A. G.; Dai, H.; Hafner, J. H.; Bradley, R. K.; Boul, P. J.; Lu, A.; Iverson, T.; Shelimov, K.; Huffman, C. B.; R-Macias, F.; Sho, Y. S.; Lee, T. R.; Colbert, D. T.; Smalley, R. E. *Science* **1998**, *280*, 1253.

(8) Thomsen, D. L.; Phely-Bobin, T.; Papadimitrakopoulos, F. *J. Am. Chem. Soc.* **1998**, *120*, 6177.

(9) (a) Galeska, I.; Chattopadhyay, D.; Moussy, F.; Papadimitrakopoulos, F. *Biomacromolecules* **2000**, *1*, 202. (b) Lvov, Y.; Ariga, K.; Onda, M.; Ichinose, I.; Kunitake, T. *Langmuir* **1997**, *13*, 6195. (c) Schenkman, J. B.; Jansson, I.; Lvov, Y.; Rusling, J. F.; Boussad, S.; Tao, N. J. *Arch. Biochem. Biophys.* **2001**, *385*, 78.

(10) DMSO suspension lead to the same results.

(11) Substrates were held normal to the base of immersion containers.

(12) NaOH titration of Fe^{3+} in DMF caused $Fe(OH)_x^{(3-x)+}$ to precipitate around pH = 5.56 followed by an instant increase of pH to 11.

(13) Muster, J.; Burghard, M.; Roth, S.; Duesberg, G. S.; Hernández, E.; Rubio, A. *J. Vac. Sci. Technol. B* **1998**, *16*, 2796.

(14) Chen, J.; Hamon, M. A.; Hu, H.; Chen, Y.; Rao, A. M.; Eklund, P. C.; Haddon, R. C. *Science* **1998**, *282*, 95.

(15) Gua, T.; Nikoleav, P.; Rinzler, A. G.; Tomanek, D.; Colbert, D. T.; Smalley, R. E. *J. Phys. Chem.* **1995**, *99*, 10694.

(16) Solid lines are linear fits for the AFM and ellipsometry data, while the broken line is used to guide the eye for the density values. The gray bars represent typical NTs size distribution at 95% weighted averages, calculated from the AFM histograms.

(17) (a) The equivalent mass was calculated using the Sauerbrey equation.[16b] (b) Sauerbrey, G. Z. *Z. Phys.* **1957**, *155*, 206.

(18) Ellipsometric and AFM values were averaged for respective immersion duration.

(19) Smith, B. W.; Benes, Z.; Luzzi, D. E.; Fischer, J. E.; Walters, D. A.; Casavant, M. J.; Schmidt, J.; Smalley, R. E. *Appl. Phys. Lett.* **2000**, *77*, 663.

(20) Li, J.; Papadopoulos, C.; Xu, J.; Moskovits, M. *Appl. Phys. Lett.* **1999**, *75*, 367.

(21) (a) Duesberg, G. S.; Muster, J.; Krstic, V.; Burghard, M.; Roth, S. *Appl. Phys A.* **1998**, *622*. (b) Duesberg, G. S.; Loa, I.; Burghard, M.; Syassen, K.; Roth, S. *Phys. Rev. Lett.* **2000**, *85*, 5436.

10.1021/ja0160243 CCC: $20.00
Published on Web 08/28/2001

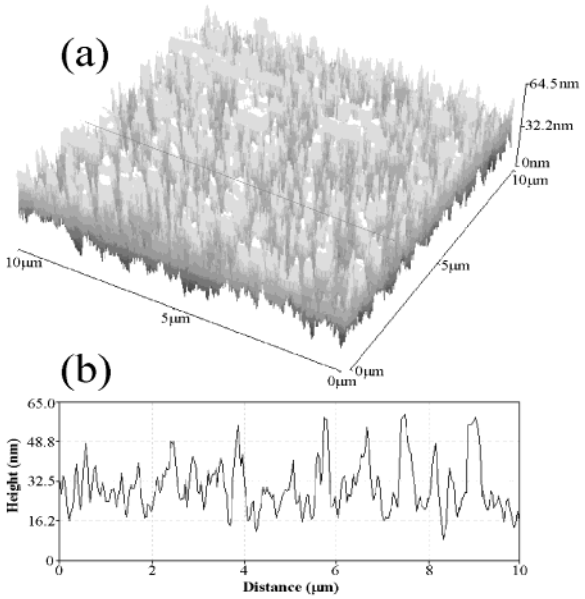

Figure 1. (a) Representative tapping-mode AFM and (b) line scan obtained after 30 min immersion of an $Fe(OH)_x^{(3-x)+}$-functionalized substrate in a DMF dispersion of s-SWNTs.

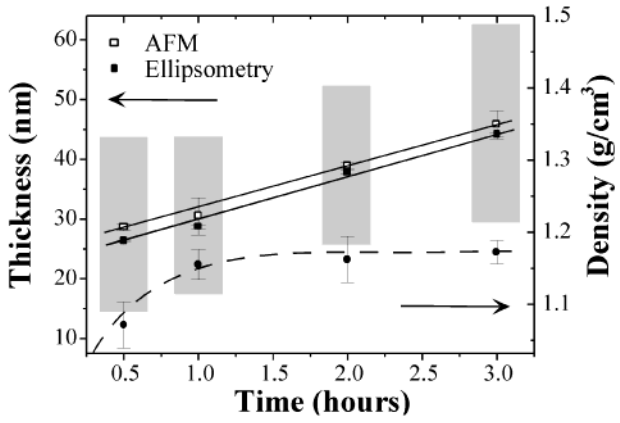

Figure 2. Average monolayer growth and film density as a function of immersion time in a 0.1 mg/mL DMF dispersion of s-SWNTs.[16]

S3 in the Supporting Information). This is further substantiated by the relatively high densities observed for these assemblies, as described below.

The left ordinate of Figure 2 depicts the average monolayer thickness as a function of immersion time in s-SWNTs dispersion, as measured by AFM[6] and spectroscopic ellipsometry.[8,9a] The apparent increase in average film thickness is accompanied by a substantial enlargement in average domain width ($\langle dw \rangle$) (as shown by domain analysis of representative AFM micrographs included in the Supporting Information). The initial needlelike features obtained from 30 min immersion ($\langle dw \rangle = 93 \pm 22$ nm) gradually broaden to $\langle dw \rangle = 387 \pm 34$ nm after 4 h. The corresponding mass deposition was monitored by the change in the resonant frequency of a QCM resonator[17] and converted to density by dividing with the average film thickness,[18] illustrated by the right ordinate axis of Figure 2. In contrast to the linear increase in film thickness and domain width, film density seems to plateau after ~1 h of immersion in s-SWNTs dispersions. These density values (1.1−1.2 g/cm^3) compare favorably with a van der Waals

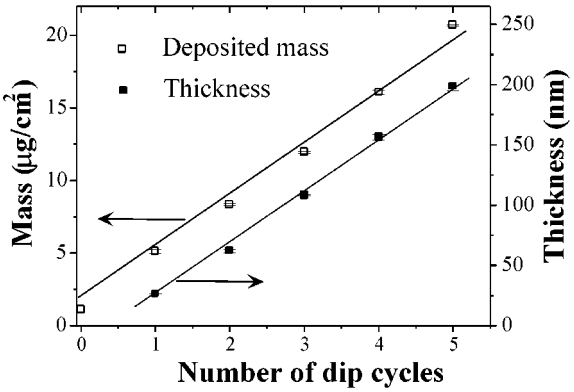

Figure 3. Multilayer growth of Fe^{3+}/s-SWNTs assemblies as a function of dip-cycles (30 min immersion in s-SWNTs dispersion).

rope-lattice SWNT crystal of 1.3−1.4 nm diameter tubes (1.33 g/cm^3),[19] indicative of a densely packed organization. For the present system s-SWNTs coverage was estimated to be on the order of 10^{13} cm^{-2}. This appears to be 2 orders of magnitude larger than those reported for NTs grown by chemical vapor deposition.[20] Thus, the increase in average thickness and domain width is most likely associated with a dynamic exchange between the shorter s-SWNTs that quickly diffuse and organize on the surface versus the longer ones, rather than a densification process. It is presently believed that the driving force for the increase in monolayer thickness and domain width might originate from enhanced hydrophobic interactions between s-SWNTs of larger-aspect ratios.

Subsequent adsorption of Fe^{3+} ions onto the carboxy-terminated s-SWNTs at the untethered ends could also facilitate the formation of multilayer Fe^{3+}/s-SWNTs assemblies. The LBL growth of such assemblies is shown in Figure 3. Both the average film thickness (measured by spectroscopic ellipsometry) and mass deposition (obtained via QCM) are in good agreement with the formation of multilayered structures, readily observed by the gradual substrate darkening. The linear increase in both average film thickness (ca. 37.7 nm) and mass (ca. 4.1 μg/cm^2) correspond to an average density of 1.1 g/cm^3 for the multilayer Fe^{3+}/s-SWNTs assemblies.

In conclusion, dense arrays of monolayer and multilayer assemblies of s-SWNTs have been demonstrated using a metal-assisted organization process from nonaqueous media. Ongoing efforts include size separation of s-SWNTs[21a] that could lead to more uniform films. Aside from their relevant importance for optoelectronic devices, these geometries could find a number of potential applications as AFM/STM probes[22a] and H_2[22b] and electrochemical energy storage.[22c]

Acknowledgment. We thank Dr. R. Baughman, A. Zakhidov, and Mr. B. Yang for helpful discussions. Financial support from NSF Career Grant DMR-970220, DARPA No. N00173-99-C-2000, and NIH No. R01RR14171 Grants is greatly appreciated.

Supporting Information Available: AFM micrographs and respective plot of average domain widths obtained for Figure 2; polarization Raman spectra for the Fe^{3+}/s-SWNTs assemblies (PDF). This material is available free of charge via the Internet at http://pubs.acs.org.

JA0160243

(22) (a)Wong, S. S.; Joselevich, E.; Woolley, A. T.; Cheung, C. L.; Lieber, C. M. *Nature* **1998**, *394*, 52. (b) Dillon, A. C.; Jones, K. M.; Bekkedal, T. A.; Kiang, C. H.; Bethume, D. S.; Heben, M. J. *Nature* **1997**, *386*, 377. (c) Che, G. L.; Lakshmi, B. B.; Fisher, E. R.; Martin, C. R. *Nature* **1998**, *393*, 346.